Plastic Deformation of Glassy Polymers: Correlation between Shear Activation Volume and Entanglement Density

Janet Ho,[†] Leon Govaert,[‡] and Marcel Utz*[,†,§]

Institute of Materials Science and Department of Physics, University of Connecticut, Storrs, Connecticut 06269, and Dutch Polymer Institute (DPI), Eindhoven University of Technology, Eindhoven, The Netherlands

Received October 11, 2002; Revised Manuscript Received June 23, 2003

ABSTRACT: The structural relaxation caused by the plastic deformation of polymer glasses is not yet fully understood. In particular, the size scale of the localized plastic relaxation events is currently unknown. In this work, the effect of molecular entanglement density on the shear activation volume of glassy polymers has been studied. The shear activation volumes of miscible polystyrene−poly(2,6-dimethyl-1,4-phenylene oxide) (PS−PPO) blends at different PS/PPO ratios have been determined experimentally by both plane-strain and uniaxial compression at constant strain rates. We find that the same correlation between the shear activation volume V^*_{eq} and the entanglement density ρ_e holds for the blend as well as for various pure glassy polymers: $V^*_{eq} = C(\rho_e/\mathrm{nm}^{-3})^{\alpha} + V_0$, with $C = 8.2 \pm 0.4$ nm^3, $\alpha = 0.6 \pm 0.03$, and $V_0 < 0.1$ nm^3. The shear activation volume is closely related to the size of the plastic shear zones; therefore, this correlation suggests that the cooperativity of the elementary processes of plastic deformation in glassy polymers scales with ρ_e.

1. Introduction

Although it is well-known that plasticity in crystalline solids results from the nucleation, mobility, and growth of lattice defects,[1] the phenomenon of plastic deformation in glassy polymers is not yet fully understood, even though many phenomenological models that accurately describe the behavior of plastic deformation in polymer glasses do exist.[2−11] Early work[12,13] postulated that the deformation in glassy polymers is comprised of dislocations that have mobility characteristics similar to those in crystalline materials; however, it is now recognized that dislocations do not govern the behavior of yielding in glassy polymers.[2] The difficulty in describing plastic deformation in glassy solids arises because the concepts of crystal plasticity[1] cannot be applied to materials that do not have long-range translational order.[2] Evidence from atomistic computer simulation studies[14−18] and calorimetric experiments[19,20] indicates that plastic deformation in glassy materials is the result of repeated nucleation of stress-relaxation events, which lead to irreversible cooperative rearrangements of molecular segments. These stress-relaxation events, which are called shear transformations, are sessile; i.e, upon nucleation, the shear transformations do not expand.[2] Therefore, the rate of plastic deformation in glassy polymers is controlled by the nucleation of shear transformations, rather than by their mobility.[2,11]

A key parameter for understanding the plasticity in glassy solids at a molecular level is the *size* of the regions in which the shear transformations occur. For polymer glasses, the length scale of these plastic shear zones (PSZs)[2] is unknown, as are the molecular parameters that control it. The purpose of this work is to explore the influence of the entanglement density (ρ_e) on the length scale of the elementary events of plastic deformation in glassy polymers.

Several theoretical models[21−24] have been proposed to describe the molecular kinematics of plastic deformation in glassy polymers. These models focus on the concept of highly localized structural change in polymer segments during plastic yielding. Eyring[21] postulated that the applied stress causes a bias to the height of the energy barrier between different stable arrangements of the molecular segments, favoring deformation in the direction of the applied stress. In the theory proposed by Robertson,[22] all backbone bonds in a polymer chain are assumed to be in either a low-energy trans state or a high-energy cis state. When stress is applied, the fraction of the cis bonds is transiently increased, which leads to an increase in the structural temperature. The polymer structure becomes "liquid-like" and, therefore, allows plastic flow to occur. With the aid of the Williams−Landel−Ferry (WLF) equation,[25] Robertson derived the plastic shear response for glassy polymers. Although Robertson's theory only considers intramolecular forces, Argon's model[23] addresses intermolecular interactions by embedding individual chains in an elastic continuum. Plastic deformation is caused by segmental rotations that are thermally activated under the applied stress to overcome the resistance that is generated from elastic interaction of the polymer chain with its surroundings.

All these ad hoc mechanisms are based on the assumption that the shear transformations are highly localized, involving only a few segments. On the other hand, atomistic computer simulation studies[15,16] have indicated rather diffuse shear transformations that involve significantly more segments. In fact, the size limitation of the simulation cells has prevented capture of the entire PSZ, and, therefore, the length scale of the PSZs is unknown. However, this length scale and the shear activation volume (V^*) are closely related, as will be discussed below. The V^* values for a few glassy polymers have been determined experimentally,[26] and

* Author to whom correspondence should be addressed. E-mail: marcel.utz@uconn.edu.
† Institute of Materials Science, University of Connecticut.
‡ Dutch Polymer Institute.
§ Department of Physics, University of Connecticut.

10.1021/ma025733d CCC: $25.00
Published on Web 00/00/0000 PAGE EST: 6.9

the sizes of the PSZs that have been calculated from these data[15] suggest that the shear transformation is significantly larger than that postulated by the previously mentioned ad hoc mechanisms.

The goal of the present work is to explore the influence of the entanglement density[27] (ρ_e) on the shear activation volume V^*. For this purpose, we have focused on miscible polystyrene−poly(2,6-dimethyl-1,4-phenylene oxide) (PS−PPO) blends. In this system, ρ_e can be varied continuously by changing the composition.[28] The shear activation volumes at different PS/PPO ratios were determined experimentally. A correlation between the V^* and ρ_e values of this blend, and of various pure glassy polymers, is demonstrated. The V^* value is closely related to the size of a PSZ; therefore, our result suggests that the length scale of the elementary processes of plastic deformation is set by the value of ρ_e.

2. Theory

A theoretical framework for plastic deformation in glassy polymers can be formulated by considering the change in the total energy of an elastic solid due to the spontaneous thermal formation of a shear transformation in the presence of an applied shear stress. Assume that an initially spherical region of volume Ω undergoes a spontaneous shear transformation of strain γ, producing an elastic stress field in its surroundings. The change in the elastic energy due to this stress field is given as[29]

$$\Delta E = \frac{7 - 5\nu}{30(1 - \nu)}\mu\gamma^2\Omega \tag{1}$$

where μ is the elastic shear modulus and ν represents Poisson's ratio. Note that, because we apply linear elasticity, ΔE does not depend on the externally applied stress. However, the shear transformation causes displacements, proportional to Ω and γ, that exert mechanical work on the external loading mechanism. This work is given by[29]

$$\Delta W = \tau\gamma\Omega \tag{2}$$

where τ is the applied stress. For a spontaneous shear transformation to lead to a plastic relaxation event, a plastic shear zone (PSZ)[2] of volume Ω_c must be deformed by at least γ^T, where Ω_c and γ^T are determined by the molecular structure of the material. Therefore, the rate of deformation is controlled by the energy barrier $\Delta H = \Delta E + \Delta W$. Taking into consideration both a positive deformation γ^T (along the applied stress) and a negative deformation (against the applied stress), this results in the Eyring flow expression:[21]

$$\dot{\gamma} = \dot{\gamma}_0 \exp\left(-\frac{\Delta E}{kT}\right) \sinh\left(\frac{\tau\gamma^T\Omega_c}{kT}\right) \tag{3}$$

where $\dot{\gamma}$ is the shear rate, $\dot{\gamma}_0$ is a prefactor, kT is the thermal energy, and all other parameters are the same as described previously. The quantity $\gamma^T\Omega_c$ is known as the shear activation volume, V^*.[7] For temperatures far below the glass transition temperature T_g, where $\tau\gamma^T\Omega_c \gg kT$, $\sinh x \approx {}^1/_2 \exp(x)$ and

$$\dot{\gamma} \approx \frac{\dot{\gamma}_0}{2} \exp\left(-\frac{\Delta E - \tau\gamma^T\Omega_c}{kT}\right) \tag{4}$$

Under the same approximation, V^* is given as the derivative of the apparent activation energy, with respect to shear stress:

$$V^* \approx \gamma^T\Omega_c = kT\frac{\partial \ln \dot{\gamma}}{\partial \tau} \tag{5}$$

Ward[30] suggested a pressure-modified version of the Eyring expression to account for the effect of hydrostatic pressure on the shear yield stress. This modification leads to the additional component of hydrostatic pressure in the shear activation volume:

$$V^* = \gamma^T\Omega_c(1 - \chi\alpha) \tag{6}$$

where χ is the coefficient of pressure dependence and α is a geometry factor that corresponds to different loading geometries. The magnitude of χ for polystyrene has been determined experimentally to be 0.1,[31] and the values of α are $\sqrt{3}/3$ for uniaxial compression and 1 for planar compression. This leads to $(1 - \chi\alpha) = 0.942$ for uniaxial compression and $(1 - \chi\alpha) = 0.9$ for planar compression. The quality of the data obtained in the present study cannot discern such a difference; therefore, the term $(1 - \chi\alpha)$ is replaced by unity in the present context.

Using eq 5, V^* can be determined experimentally from stress−strain data. To gain insight into the molecular nature of the deformation process, it would be of interest to know γ^T and Ω_c independently. Current computer simulation evidence suggests that the value of γ^T is universally ~0.02 for amorphous polymers.[15] As more data become available, particularly from simulations with larger cell sizes, this point may need to be revisited.

The primary objective of the present work was to explore the influence of the entanglement density ρ_e, which is a key structural parameter of amorphous polymers, on the shear activation volume V^*. Intuitively, one would expect the elementary relaxation processes upon deformation to be more collective (larger Ω_c) for a more highly entangled polymer. Together with the assumption of a universal value for γ^T, this leads to the expectation of a positive correlation between ρ_e and V^*.

The present work focuses on the well-known polystyrene−poly(2,6-dimethyl-1,4-phenylene oxide) (PS−PPO) polymer blend system.[32] This blend is miscible at all compositions, and the ρ_e values of the pure components differ by a factor of 5. The ρ_e value of the blend can be adjusted in the same range by varying the composition.

3. Experimental Section

Blends of polystyrene (PS) and poly(2,6-dimethyl-1,4-phenylene oxide) (PPO) were prepared using coprecipitation and melt blending. Three PS−PPO polymer blends (PS molecular weight (M_w) of 280 000 g/mol, PPO M_w = 244 000 g/mol; both from Aldrich Chemical Co.)—with 25, 50, and 75 wt % PPO—were prepared using the following coprecipitation technique. An appropriate amount of each polymer was dissolved in chloroform (HPLC grade) to give a 3 wt % polymer solution, which was stirred at room temperature for 24 h. The resulting polymer blend then was precipitated in a 10-fold volume of methanol (certified ACS grade), and the polymer was separated from the solvent by vacuum filtration. The collected polymer was dried under vacuum at 333 K for >48 h. For pure PS, the pellets were first dissolved in the same solvent, and the polymer was harvested using the same procedure. The homogeneity of the polymer blend was confirmed using a Perkin−Elmer differential scanning calorimeter. A single glass transition was

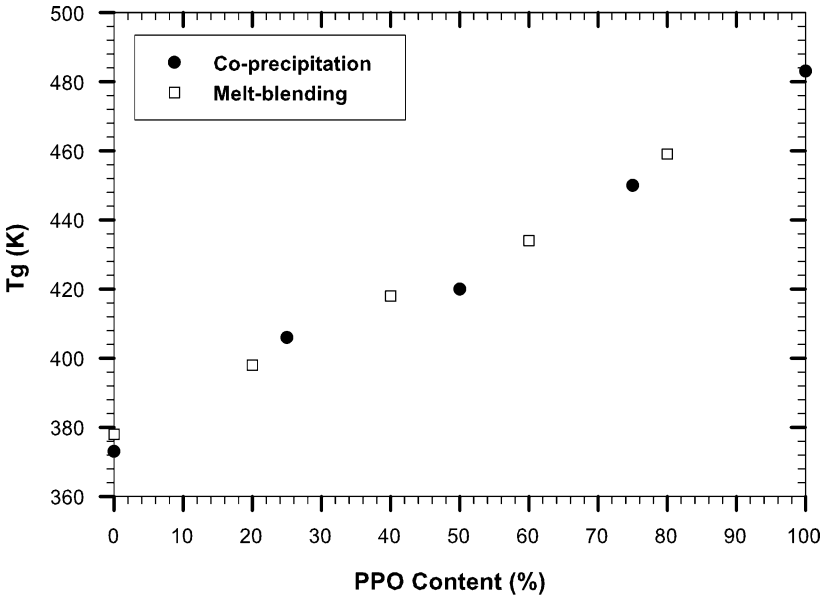

Figure 1. Glass transition temperature (T_g) of each composition (wt %) of PS−PPO blend measured on a differential scanning calorimeter (Perkin−Elmer model DSC 7) at a heating rate of 20.0 °C/min in a nitrogen atmosphere, using polymer specimens with a mass of 10−20 mg.

observed in all cases. Melt-blended PS−PPO samples (the PS component was Styron 638, from Dow Chemical Company, The Netherlands, and the PPO component was PPO 803, from General Electric Plastics, The Netherlands) were obtained from General Electric Plastics. The measured T_g of each composition is shown in Figure 1.

From the blends prepared by coprecipitation, rectangular samples for plane-strain compression experiments were compression-molded in a steel die with ground surfaces. The polymer was first heated in the die to a temperature 50 K above T_g for 7 min with no load. A pressure of 190 MPa then was applied, and the sample was allowed to cool to room temperature for 20 min. The final dimensions of the rectangular samples were 8 mm × 3 mm × 6 mm (length (l) × width (w) × height (h)). The samples showed no inhomogeneity upon inspection between crossed polarizers.

For the melt-blended polymers, the granular material was molded into plates using two different methods. In molding method I, the granular material was compression-molded, stepwise, into plates 9 mm thick. The material was first heated in a mold with dimensions of 160 mm × 160 mm to 80−90 K above T_g for 15 min. Next, the material was compressed in the mold at the same temperature in five steps of increasing pressure, up to 12 MPa, over a period of 5 min. The pressure was released between these steps to allow degassing. The mold was then placed into a cold press and cooled to room temperature at a pressure of 4 MPa. From these plates, rectangular bars with a cross-sectional area of 9 mm × 9 mm were cut, from which cylindrical samples with dimensions of 6 mm × 6 mm were machined for uniaxial compression experiments. In molding method II, 30 g of the granular material was first homogenized into a single mass, using a Brabender Prep-center that had been fitted with roller blades and a 30-mL bowl, at a temperature 60 K above T_g and a speed of 30 rpm for 3 min. The single mass was then heated in a mold with dimensions of 42 mm × 66 mm × 8 mm (l × w × d) to 80 K above T_g for 15 min. The material then was compressed in the mold to a thickness of 4 mm at a pressure of 10 MPa for 5 min and was cooled to room temperature over a period of 10 min. Rectangular samples with dimensions of 8 mm × 3 mm × 6 mm (l × w × h) were machined from these slabs for plane-strain compression experiments.

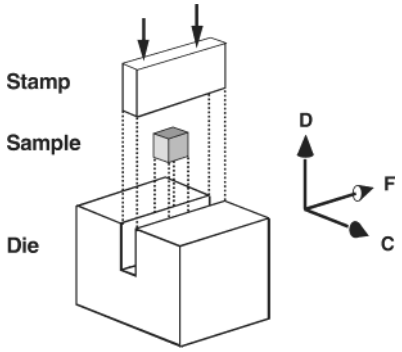

Figure 2. Schematic drawing of a plane-strain compression experiment by means of a channel die. The entire setup is mounted onto a mechanical testing machine, and the sample is extruded by means of a stamp. The deformation geometry is characterized by three directions: F (free), C (constraint), and D (deformation).

Plane-strain compressive deformation was performed by means of a channel die that was fixed onto an Instron model 8500 mechanical testing unit. Figure 2 illustrates the testing geometry. The channel die was jacketed with a circulating water bath that was maintained at a temperature of 297.0 ± 0.2 K. To reduce friction, the samples were wrapped in a thin layer of poly(tetrafluoroethylene) (PTFE) tape, and surfaces between the tape and the channel die were lubricated with a soap−water solution.[33] The deformation experiments were conducted at strain rates of 3.0×10^{-4}, 6.0×10^{-4}, 1.2×10^{-3}, 2.4×10^{-3}, 4.8×10^{-3}, and 9.6×10^{-3} s^{-1}. Three samples were tested at each strain rate. A computer program was used to control the Instron testing machine by continuously adjusting the velocity of the actuator such that the separation between the stamp and the die followed an exponential decay, thus ensuring a constant

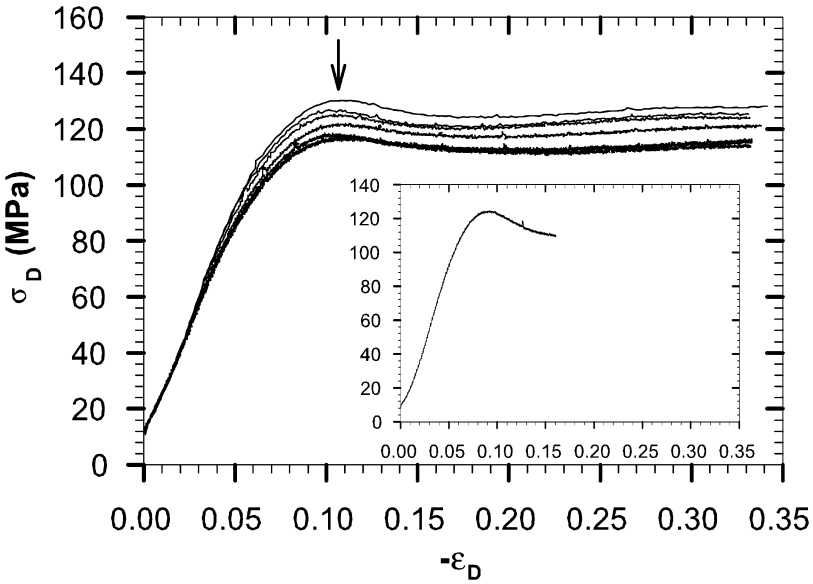

Figure 3. True stress−strain curves of a coprecipitated 40/60 PPO blend, which resulted from plane-strain compression by means of a channel die at various strain rates. Strain rates (curves from top to bottom) are 9.6×10^{-3}, 4.8×10^{-3}, 2.4×10^{-3}, 1.2×10^{-3}, 6.0×10^{-4}, and 3.0×10^{-4}. Arrow indicates the yield stress. Inset shows the pre-deformation to a strain of 0.16 at a strain rate of 3.0×10^{-4}.

logarithmic strain rate.[33] True stress, as a function of true strain, was recorded. The data were corrected for the finite compliance of the experimental setup, which was measured by running an experiment with an empty channel die. Immediately prior to the actual measurement, each sample was pre-deformed to a strain of 16%, using the slowest strain rate, to erase the thermomechanical history. After the pre-deformation treatment was completed, the load was released and the actual deformation experiment with a prescribed strain rate began immediately.

Uniaxial compression tests were performed on a servo-hydraulic testing system (MTS Elastomer Testing System model 810). Cylindrical samples were compressed between two parallel, flat steel plates at constant logarithmic strain rates of 10^{-3}, 10^{-2}, and 10^{-1} s^{-1}. All tests were conducted at a temperature of 298.0 ± 0.5 K, which was controlled by placing the entire setup in a temperature chamber that was cooled with liquid nitrogen. To ensure a thermal equilibrium at the desired temperature, the sample was mounted in the setup 15 min prior to the testing. The applied method for lubrication was the same as that previously described. The aging history of the samples was erased by heating to 10 K above T_g, followed by rapid quenching. During the compression test, no bulging or buckling of the sample was observed, indicating that the friction was sufficiently reduced. The relative displacement of the steel plates was recorded by an extensometer (Instron model 2630-111). Both displacement and force were recorded by data acquisition at an appropriate sampling frequency that was dependent on the strain rate such that a minimum of 1000 data points were collected per test.

4. Results and Discussion

To be able to compare results from different testing geometries, the yield stress in the deformation direction, σ_D, which was obtained from the maximum of a true stress−true strain curve, was converted to the equivalent shear stress at the yield point, τ_{eq}. Figure 3 illustrates an example of a full set of stress−strain curves. τ_{eq} is defined as the second invariant of the stress tensor σ:

$$\tau_{eq} = \sqrt{\frac{1}{6}[(\sigma_1 - \sigma_2)^2 + (\sigma_2 - \sigma_3)^2 + (\sigma_3 - \sigma_1)^2]} \quad (7)$$

where σ_i are the principal stresses. For uniaxial compression, $\tau_{eq} = \sigma_D/\sqrt{3}$, whereas for plane-strain compression, under the assumption of elastic isotropy and a Poisson's ratio of $\nu = 0.4$, $\tau_{eq} = 0.50\sigma_1$. All results in the remainder of this paper are given in terms of τ_{eq}. Figure 4 shows the equivalent yield stress as a function of PPO content. The yield stress increases steadily up to a PPO content of 60%, where it reaches a maximum. The dependence of the yield stress on the strain rate decreases monotonically as the PPO content increases.

The shear activation volume V^*_{eq} was obtained from linear regression of the natural logarithm of the shear rate, as a function of the von Mises equivalent yield stress, as illustrated in Figure 5. The results for melt-blended and coprecipitated blends, obtained from uniaxial and plane-strain compression, are summarized in Figure 6. The value of V^*_{eq} increases from ~1.5 nm^3 for pure PS to 3.3 nm^3 for pure PPO. The large error bars observed in the coprecipitated samples may result from variability among the individually molded samples. The scatter is much smaller in the case of the melt-blended samples, which were cut from a single molded plate (Figure 5). Note that our results, which were obtained independently in two separate laboratories, seem to conflict with the results of Creton et al.,[34] who found the activation volume to be independent of composition.

As shown in Figure 7, the activation volumes of the blends under study here, as well as those of other glassy polymers, fall onto the same master curve if plotted asa function of the entanglement density ρ_e. The entanglement density of a polymer is given as

$$\rho_e = \frac{\rho N_A}{M_e} \quad (8)$$

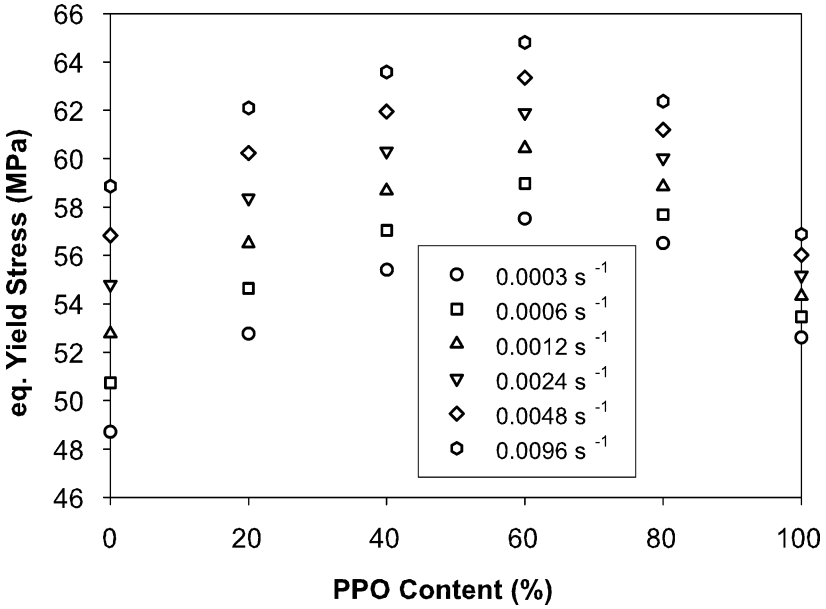

Figure 4. Equivalent yield stress for various PS−PPO blends, as a function of PPO composition. Yield stress is taken as the maximum of a true stress−true strain curve.

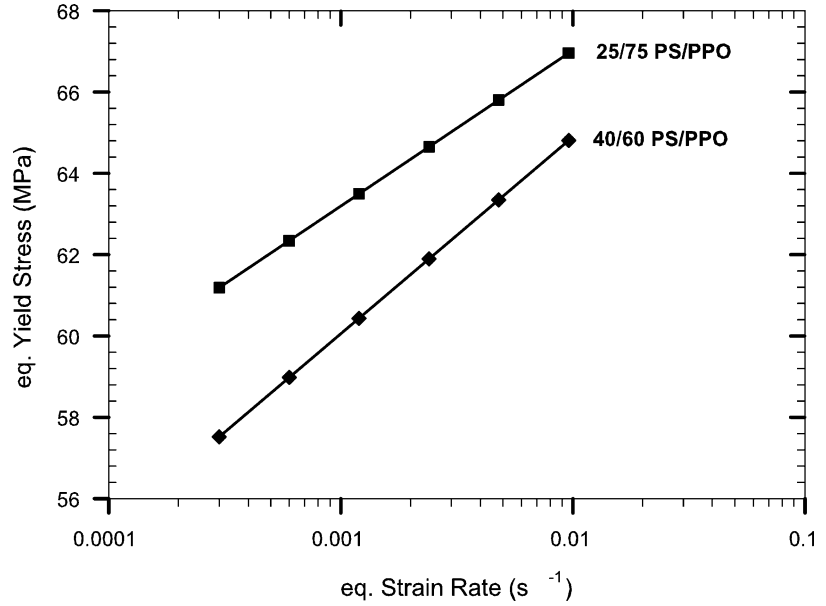

Figure 5. Equivalent shear stress as a function of equivalent strain rate from plane-strain compression of PS−PPO blends: (■) blends prepared by coprecipitation and (◆) blends made by melt blending and compression-molded using method II. Solid lines show the linear regressions.

where ρ is the mass density, N_A denotes Avogadro's number, and M_e is the molecular weight between entanglements. Values of ρ_e for pure polymers, including PS and PPO, were determined from the plateau moduli given by Fetters et al.[35] For the blends, ρ_e was calculated by employing the mixing rule that was proposed by Tsenoglou[36] originally for the plateau modulus, G_N^0:

$$(G_N^0)_b^{1/2} = \phi_1(G_N^0)_1^{1/2} + \phi_2(G_N^0)_2^{1/2} \qquad (9)$$

where ϕ is the volume fraction and the subscripts b, 1, and 2 represent the blend and the two pure components, respectively. This mixing rule is based on the random formation of entanglements between chains of the two components. Lomellini[28] showed that the PS−PPO blend system obeys this mixing rule to good precision over the entire range of compositions. The entanglement density ρ_e is proportional to the plateau modulus G_N^0;[37] therefore, it must also follow this mixing rule.

The results shown in Figure 7 clearly suggest a correlation between the shear activation volume V_{eq}^* and the entanglement density ρ_e. V_{eq}^* and the size of a PSZ, Ω_c, are closely related (cf eq 6). The same transformation shear strain, $\gamma^T \approx 0.02$, has been found in computer simulation studies of the plastic deformation of both atactic polypropylene[15] and polycarbonate,[16] despite the higher chain stiffness in the latter. Therefore, it has been concluded tentatively that different polymers have the same, or at least similar, transformation shear strains. In view of this hypothesis, the correlation demonstrated in this contribution suggests that the size of the PSZs increases systematically as the ρ_e value of the polymers increases. It seems intuitive that a more highly entangled polymer should

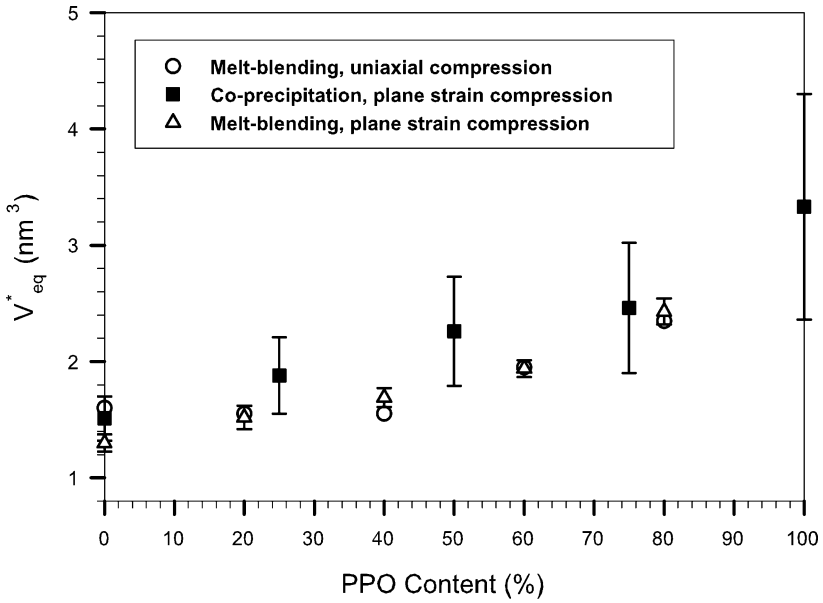

Figure 6. Shear activation volume of PS/PPO blend (V^*_{eq}), as a function of PPO composition. Open symbols represent melt-blended PS−PPO blend (circles represent uniaxial compression samples made from molding method I, and triangles represent plane-strain compression samples made from molding method II). Filled squares denote coprecipitated PS/PPO blends in plane-strain compression.

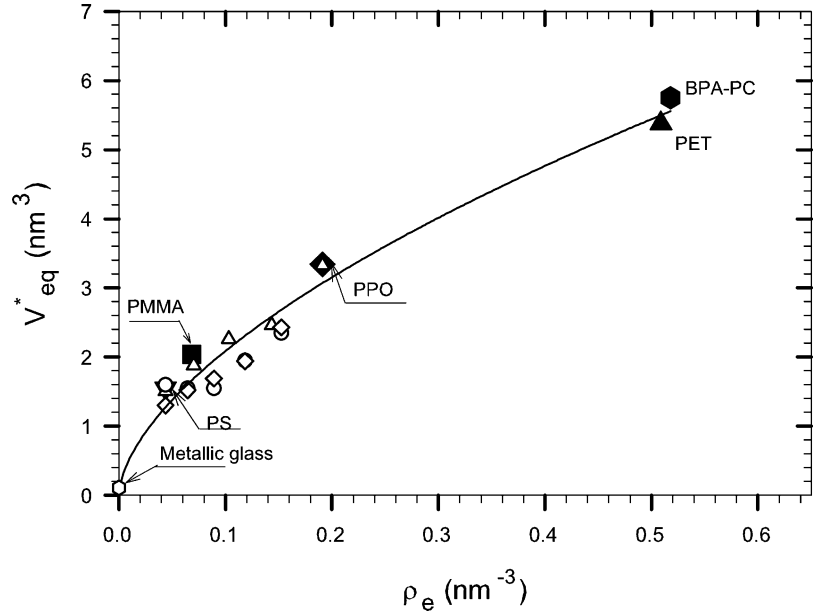

Figure 7. Correlation between the shear activation volume V^*_{eq} and the entanglement density ρ_e of glassy materials. Solid symbols denote V^*_{eq} data from ref 15 and ρ_e data from ref 35. PS, polystyrene; PMMA, poly(methyl methacrylate); PPO, poly(2,6-dimethyl-1,4-phenylene oxide); PET, poly(ethylene terephthalate); and BPA-PC, bisphenol A polycarbonate. Legend: (⬡) V^* of metallic glass $Pd_{80}Si_{20}$ (from ref 38); (△) coprecipitated PS−PPO blend, plane-strain compression (from present study); (○) melt-blended PS−PPO blend (molding method I), uniaxial compression (from present study); and (◇) melt-blended PS−PPO blend (molding method II), plane-strain compression (from present study)). The solid line is a power-law fit to the data. A scaling factor of 0.3 has been applied to the shear activation volumes reported in ref 15, to account for a different definition of V^*.

exhibit more cooperative elementary plastic events and, thus, a larger V^*_{eq} value. However, to our knowledge, there is currently no formal theory that predicts the observed correlation between V^*_{eq} and ρ_e.

As shown in Figure 7, the data are well represented by the power law

$$V^*_{eq} = C\left(\frac{\rho_e}{\mathrm{nm}^{-3}}\right)^{\alpha} + V_0 \qquad (10)$$

with $C = 8.2 \pm 0.4$ nm^3 and $\alpha = 0.6 \pm 0.03$ (error margins represent one standard error of fit). V_0, which represents the residual activation volume in the absence of entanglements, is not determined reliably by our data. We can only indicate an upper bound of $V_0 < 0.2$ nm^3. By comparison, the activation volume of the metallic glass $Pd_{80}Si_{20}$ has been determined to be 0.11 nm^3.[38] Alternatively, the data can be represented by a straight line with a slope of 9.1 ± 7.0 nm^3 and an intercept of 1.0 ± 0.7 nm^3; however, the quality of fit is noticeably worse than for the power law. Our results indicate that ρ_e has a crucial role in the initial stages of plastic deformation and suggest that the yield behavior of polymers below the glass transition may be

predicted by ρ_e. Both the strain hardening at large homogeneous deformations[3] and the crazing behavior[39,40] have been shown to be related to the existence of molecular entanglements. In the latter case, it has been shown that the extension ratio in the craze fibrils directly reflects the maximum extension warranted by the entanglement density in PS−PPO blends of various compositions.[41] Similar studies on chemically cross-linked polystyrene have confirmed that the fibril extension ratio is really controlled by the topological constraints that are caused by molecular entanglement.[42] The results presented in this paper are suggestive of a similarly important role of the topological entanglement constraints in determining the size scale of the elementary processes of plastic deformation.However, note that the entanglement density ρ_e is controlled by the molecular geometry and stiffness.[35] Therefore, the correlation between ρ_e and V^* might not be due to a direct causal link. Instead, both quantities might be dependent on the molecular geometry in a similar way. Experiments on chemically cross-linked polymers will be very helpful in clarifying this point.

5. Conclusions

In summary, a universal correlation between the shear activation volumes and the entanglement densities of the miscible polystyrene−poly(2,6-dimethyl-1,4-phenylene oxide) (PS−PPO) polymer blend system and those of various pure glassy polymers has been demonstrated. The shear activation volumes of the polymer blends at different PS/PPO ratios were determined experimentally from plane-strain and uniaxial compression. Our result suggests that the cooperativity of the elementary processes in plastic deformation scales with the entanglement density in glassy polymers. Whether this is due to a direct role of the topological entanglement constraints in plastic deformation remains an open question, which may be clarified by future experiments on chemically cross-linked samples.

Acknowledgment. This work has been supported through an Early Career Development Award to M.U. by the National Science Foundation (DMR-0094290), and through a Junior Faculty Grant from the Petroleum Research Fund, administrated by the American Chemical Society. We thank Mr. V. Dutot for his help in constructing the channel die apparatus.

References and Notes

(1) Cottrell, A. H. *Dislocations and Plastic Flow in Crystals*; Clarendon Press: Oxford, U.K., 1953.
(2) Argon, A. S. Inelastic Deformation and Fracture of Glassy Solids; Materials Science and Technology: A Comprehensive Treatment, Vol. 6, *Plastic Deformation and Fracture of Materials*; VCH: Weinheim, Germany, 1993; pp 462−508.
(3) Arruda, E. M.; Boyce, M. C. *Int. J. Plast.* **1993**, *9*, 697−720.
(4) Arruda, E. M.; Boyce, M. C.; Quintus-Bosz, H. *Int. J. Plast.* **1993**, *9*, 783−811.
(5) Arruda, E. M.; Boyce, M. C. *J. Mech. Phys. Solids* **1993**, *41*, 389−412.
(6) Arruda, E. M.; Boyce, M. C.; Jayachandran, R. *Mech. Mater.* **1995**, *19*, 193−212.
(7) Ward, I. M. *Mechanical Properties of Solid Polymers*, 2nd ed.; Wiley: Chichester, U.K., 1990.
(8) Tervoort, T. A.; Klompen, E. T. J.; Govaert, L. E. *J. Rheol.* **1996**, *40*, 779−797.
(9) Spathis, G.; Kontou, E. *J. Appl. Polym. Sci.* **1999**, *71*, 2007−2015.
(10) Tervoort, T. A.; Govaert, L. E. *J. Rheol.* **2000**, *44*, 1263−1277.
(11) Spathis, G.; Kontou, E. *J. Appl. Polym. Sci.* **2001**, *79*, 2534−2542.
(12) Gilman, J. J. In *Dislocation Dynamics*; Rosenfield, A. R., Hahn, G. T., Bement, A. L., Jaffee, R. I., Eds.; McGraw−Hill: New York, 1968; p 3.
(13) Li, J. C. M. *Distinguished Lectures in Materials Science*; Marcel Decker: New York, 1974.
(14) Deng, D.; Argon, A. S.; Yip, S. *Philos. Trans. R. Soc. London A* **1989**, *329*, 549−573, 575−593, 595−612, 613−640.
(15) Mott, P. H.; Argon, A. S.; Suter, U. W. *Philos. Mag. A* **1993**, *67*, 931−978.
(16) Hutnik, M.; Argon, A. S.; Suter, U. W. *Macromolecules* **1993**, *26*, 1097−1108.
(17) Maeda, K.; Takeuchi, S. *Philos. Mag. A* **1981**, *44*, 643−656.
(18) Srolovitz, D.; Vitek, V.; Egami, T. *Acta Metall.* **1983**, *31*, 335−352.
(19) Oleynik, E. F.; Rudnev, S. N.; Salamatina, O. B.; Topolkaraev, V. A. *Makromol. Chem., Macromol. Symp.* **1992**, *53*, 77−80.
(20) Oleynik, E. F.; Salamatina, O. B.; Rudnev, S. N.; Shenogin, S. V. *Polym. Adv. Technol.* **1995**, *6*, 1−9.
(21) Halsey, G.; White, H. J.; Eyring, H. *Text. Res. J.* **1945**, *15*, 295−311.
(22) Robertson, R. E. *J. Chem. Phys.* **1966**, *44*, 3950−3956.
(23) Argon, A. S. *Philos. Mag.* **1973**, *28*, 839−865.
(24) Yannas, I. V.; Luise, R. R. In *The Strength and Stiffness of Polymers*; Zachariades, R. E., Porter, R. S., Eds.; Marcel Dekker: New York, 1983.
(25) Williams, M. L.; Landel, R. F.; Ferry, J. D. *J. Am. Chem. Soc.* **1955**, *77*, 3701.
(26) Argon, A. S.; Hannoosh, J. G. *Philos. Mag.* **1977**, *36*, 1195−1216.
(27) Graessley, W. W. *Adv. Polym. Sci.* **1974**, *16*, 1.
(28) Lomellini, P. *Macromol. Theory Simul.* **1994**, *3*, 567−574.
(29) Eshelby, J. D. In *Progress in Solid Mechanics*; Sneddon, I. N., Hill, R., Eds.; North-Holland: Amsterdam, 1961; Vol. 2, pp 87−140.
(30) Ward, I. M. *J. Mater. Sci.* **1971**, *6*, 1397−1417.
(31) Tervoort, T. A. Constitutive Modelling of Polymer Glasses. Ph.D. Thesis, Technical University Eindhoven, The Netherlands, 1996.
(32) Cizek, E. P. U.S. Patent 3,383,435, 1968.
(33) Boyce, M. C.; Arruda, E. M. *Polym. Eng. Sci.* **1990**, *30*, 1288−1298.
(34) Creton, C.; Halary, J.; Monnerie, L. *Polymer* **1998**, *40*, 199−206.
(35) Fetters, L.; Lohse, D.; Richter, D.; Witten, T.; Zirkel, A. *Macromolecules* **1994**, *27*, 4639−4647.
(36) Tsenoglou, C. *J. Polym. Sci., Part B: Polym. Phys.* **1988**, *26*, 2329−2339.
(37) Graessley, W. W. *J. Polym. Sci., Part B: Polym. Phys.* **1980**, *18*, 27−34.
(38) Argon, A. S.; Shi, L. T. *Acta Metall.* **1983**, *31*, 499−507.
(39) Donald, A. M.; Kramer, E. J.; Bubeck, R. A. *J. Polym. Sci. Polym. Phys.* **1982**, *20*, 1129−1141.
(40) Lin, J.-H.; Yang, A. C.-M. *Macromolecules* **2001**, *34*, 3698−3705.
(41) Donald, A. M.; Kramer, E. J. *Polymer* **1982**, *23*, 461−465.
(42) Henkee, C. S.; Kramer, E. J. *J. Polym. Sci. Polym. Phys.* **1984**, *22*, 721−737.

MA025733D